

# Temperature Monitoring in Tissue Phantoms via Spatially Resolved Measurement of Longitudinal Wave Speed

Mario Wolf, Lukas Timmermann, André Juhrig,  
Katharina Rath, and Elfgard Kühnicke

Solid State Electronics Laboratories  
Technical University of Dresden  
Dresden, Germany  
Email: mario.wolf@tu-dresden.de

Felix Krujatz

Institute of Natural Materials Technology  
Technical University of Dresden  
Dresden, Germany  
Email: felix.krujatz@tu-dresden.de

**Abstract**—To optimize hyperthermia in cancer therapy, a monitoring of temperature in the tumor and in the surrounding tissue is necessary during the therapy. As the use of Computer Tomography (CT) or Magnetic Resonance Imaging (MRI) is hardly possible during the operation, ultrasonic measurements serve as a very good alternative. This contribution introduces a method to measure the longitudinal wave speed spatially resolved by analyzing the reflected ultrasonic signals from small scatterers in a tissue phantom without needing any large reflectors at known positions. The measurements are done with pre-focused annular-arrays and the recorded signals are focused synthetically. This allows to determine the resulting signal amplitude in a fixed time window as a function of the assumed longitudinal wave speed used for focusing. The amplitude becomes maximal if the assumed sound velocity is equal to the actual one. Sliding the analysis window through the whole signal allows to determine the mean longitudinal wave speed for each depth. As the longitudinal wave speed depends on temperature, this gives the temperature distribution along the acoustic axis of the transducer. To qualify the technique, measurements are done on a tissue phantom for constant sound velocity. The capabilities of the method are demonstrated by monitoring the temperature distribution during local heating of a tissue phantom. Additionally, the reachable accuracy, as well as reachable temporal and local resolution are discussed.

**Keywords**—Ultrasound; Temperature Monitoring; Annular Arrays; Tissue phantoms.

## I. INTRODUCTION

Hyperthermia for cancer therapy is a promising alternative to the widely spread radio- or chemotherapy [1]. It works by thermal destruction of the tumour, e.g., by High Intensity Focused Ultrasound (HIFU) or radio frequency ablation. A minimal temperature of 45 °C to 63 °C (according to literature [2][3]) is necessary for a successful therapy. Whereas the temperature in the surrounding tissue should be as low as possible to avoid tissue injury. Especially if there are vessels near the tumour they cause a heat transport resulting in a too low temperature in the tumour and a possible heat accumulation in other tissue. Due to these complications, a temperature monitoring during the hyperthermia surgery is needed. Although imaging techniques like CT or MRI can be used to determine a temperature distribution, they are hardly applicable during the surgery. So, ultrasound is the preferred method.

The classical approach to monitor temperature changes evaluates the displacement of scatterers in the tissue caused

by thermal expansion [4]. This approach has some significant drawbacks: First, the sound velocity increases with temperature, which reduces the time of flight of the echo of one reflector. In opposite, the thermal expansion increases the distance and thereby the time of flight. This reduces the sensitivity and in worst case, there is no change in time of flight with a change in temperature. Second, the thermal expansion coefficient is unknown and there is a large variation not only between different types of tissue but also individual. This results in a temperature distribution localised at a wrong position.

This contribution introduces an approach to monitor the temperature distribution within a tissue phantom. Evaluating the backscattered echoes gained with an annular array, allows a synthetic focussing to determine the longitudinal wave velocity within the phantom locally resolved. As this sound velocity is a function of temperature, the temperature distribution can be determined from the sound velocity profile.

Note that in this contribution sound velocity always means the longitudinal wave speed. Effects of denaturation, which also change the longitudinal wave speed are neglected and will be the objective of future work. Section II describes the used experimental set-up, Section III explains the developed measuring technique and Section IV gives the results of the experiments. Finally, Section V concludes the paper and gives perspectives for future work.

## II. EXPERIMENTAL SET-UP

Preliminary examination had been necessary to develop a tissue phantom with acoustic properties similar to tissue, which models the scattering of tissue and which also changes its properties with increasing temperature, when denaturation occurs in tissue. To develop the measuring technique material with stable and reproducible properties had been required, so that using real tissue was not possible. As bulk material we selected a gel of 5%-polyacrylamide, consisting of 26.9% acrylamide, 1.4% bisacrylamide, 71.7% water or egg-white as well as ammonium persulphate and *N, N, N', N'*-Tetramethylethylenediamine to start polymerisation. As scattering particles we use *Chlorella Vulgaris*, a robust monocellular green algae, which can be cultivated easily. The resulting gel-phantom is placed in a water basin where it can be heated and where the ultrasonic measurements can be performed. Figure 1 shows a Cross section of algae in the gel, obtained with an optical microscope.

Figure 2 shows the basic set-up with the gel (left) in a water basin and the ultrasound annular array (right). For data acquisition, a measuring board with 8 channels, a sampling rate of 125 MS/s and a samplesize of 14 bit is used.

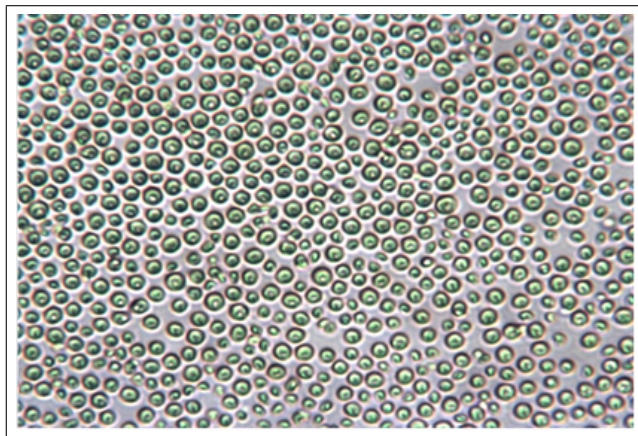


Figure 1. Cross section of the algae in the polyacrylamide-gel, obtained with an optical microscope.

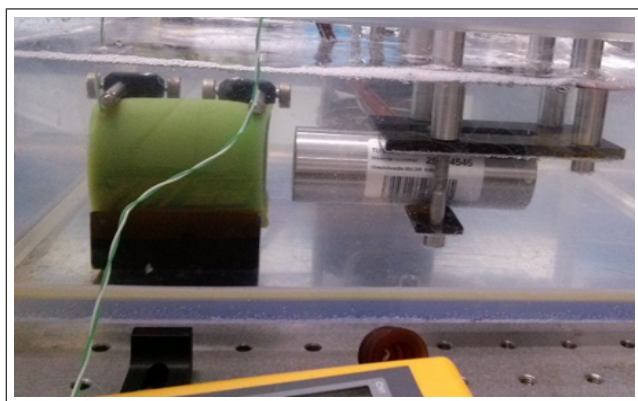


Figure 2. Experimental set-up with gel (left, green) in a water basin and the used annular array, on the right.

A custom-made annular array with a centre frequency of 10 MHz is used. Its structure has been optimized for the measurements and it has been developed for high temperatures as the common ones would not resist them. Figure 3 shows the structure of the array. The whole piezoelectric material is curved spherically with a radius of curvature of 50 mm. All elements have the same active area, and so their natural focus is in the same depth. This is necessary for effective focussing. The inner and outer radii as well as the  $r$  and  $z$  coordinates, used for focussing, see (2), are given in Table I. Also, the central element is a ring because there is a tube along the rotation axis of the transducer. For some experimental set-ups, gas, which was solved in the water, cumulates in the curvature of the transducer during the heating. The tube can be used to pump off this gas.

If the phantom is placed in a water basin, it can be heated only to an overall temperature, independent of location. An alternative set-up, which allows to generate a temperature gradient, is shown in Figure 4. At the bottom, there is a basin

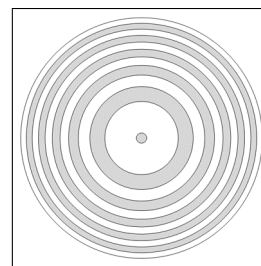


Figure 3. Structure of the used annular array; white: active area, grey: passive area.

TABLE I. RADII OF THE RINGS OF THE ANNULAR ARRAY.

Element-No.	1	2	3	4	5	6
$r_i$ [mm]	0,5	5,05	7,13	8,72	10,07	11,25
$r_a$ [mm]	3,59	6,18	7,96	9,42	10,68	11,80
$r_{eff}$ [mm]	2,56	5,64	7,56	9,08	10,38	11,53
$z_{eff}$ [mm]	0,07	0,32	0,57	0,83	1,09	1,37

with water, which is kept at a temperature of 4 °C. A second basin filled with the phantom material is placed above. It has a baseplate of metal for a good thermal coupling. On the top, there is a heating surface with a small hole in the middle, where the array can be placed. As the lateral dimensions are much larger than the height of the set-up (diameter of 20 cm and height of 6 cm), a one-dimensional temperature distribution can be assumed near the rotation axis of the gel.

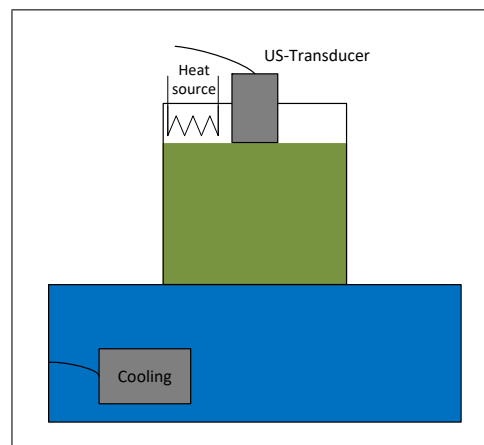


Figure 4. Schematic depiction of the experimental set-up to generate an temperature gradient. There is a cooling at the bottom and a heating surface at the top.

### III. MEASURING METHOD

To evaluate the measured data, synthetic focussing is used. This means that each element is driven separately and the reflected wave is recognized on each element. The resulting signal for each element is digitized and stored separately. Although this reduces the signal to noise ratio, it can be used to superpose the recorded signals afterwards, whereby the delay times between the signals can be chosen arbitrarily.

Figure 5 shows an example a signal by emitting and receiving with the central element, averaged over 1000 signals to improve the signal-to-noise ratio (SNR). At the top, the

whole signal is shown, including the surface echo from water to gel ( $42 \mu s$ ), the back-wall echo from gel to aluminium ( $105 \mu s$ ) and a multiple reflection in the aluminium plate ( $118 \mu s$ ). Figure 5 (bottom) shows a zoom on the surface echo. Whereas there are no previous echoes, there can be seen many echoes after the surface echo. These echoes are backscattered from the algae. Similar signals are obtained for all 36 combinations of emitters and receivers.

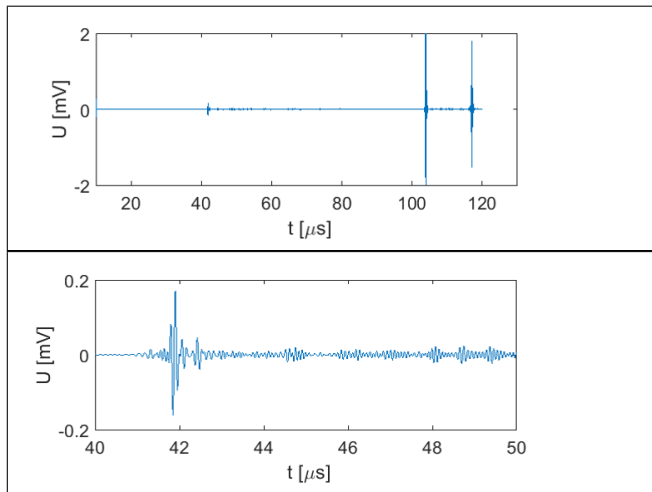


Figure 5. Recorded signal by emitting and receiving with the central ring; top: whole echo including surface echo and back-wall echoes; bottom: signal part including surface echoes and backscattered echoes from the algae

For the following considerations, it shall be assumed that the amplitude of the wave, backscattered from an algae, is proportional to the amplitude of the incident wave. The amplitude becomes maximal if the focus is located at the scatterer.

Figure 7 shows the calculated sound fields for focussing in to different depth, to  $35 \text{ mm}$ , at the top and to  $45 \text{ mm}$  at the bottom. Different focussing regimes are used:

- left:  $c_{Med} = c_{Fok}$ , focussing works correctly;
- middle: using focussing regime for  $c_{Fok} = 1200 \text{ m/s}$  in the same medium, resulting focus is too near at the transducer,
- right: focussing with the same regime as at the left, but in a medium with  $c_{Med} = 1200 \text{ m/s}$ , focus shifts away from transducer

As Figure 7 shows, the resulting focus of an annular array depends on the transducer geometry, the sound velocity of the propagation medium and the used set of delay times and it shows that focussing only works correctly, if the sound velocity used for focussing is similar to the one of the medium.

So, the goal is to find that set of delay times for focussing where the resulting signal amplitude becomes maximal. How the sound velocity is connected to the set of focussing times is described in the following section.

#### A. Synthetic Focussing

Synthetic focussing means that the signals are superposed with an arbitrary delay time.

$$S_{Fok} = \sum_{n=1}^6 \sum_{m=1}^6 S_{mn}(t - \Delta t_m - \Delta t_n + 2\Delta t_1) \quad (1)$$

where  $S_{mn}$  is the signal emitted from element  $m$  and received from element  $n$ . As the signals are obtained by scattering and not by a specular reflection, it is sufficient to calculate the different propagation path lengths from each element to an arbitrary assigned focus point on the acoustic axis of the array and dividing the differences by the sound velocity. The different propagation paths are illustrated in Figure 6.

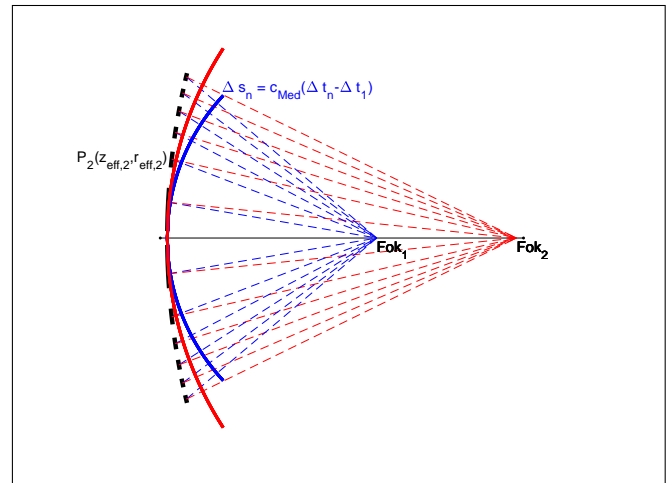


Figure 6. Illustration of the path length differences to generate a virtual curvature.

$$\Delta t_n = \frac{\sqrt{(z_{Fok} - z_{eff,n})^2 + r_{eff,n}^2}}{c_{Med}} \quad (2)$$

with  $z_{eff,n}$  and  $r_{eff,n}$  are the coordinates, which are used for ring no.  $n$ . They are given in Table I. The resulting times are accumulated in a matrix: the focussing regime  $F$ , which only depends on the assigned focus point  $z_{Fok}$  and the used (assumed) sound velocity  $c_{Fok}$ .

$$F(z_{Fok}, c_{Fok}) = [\Delta t_1, \Delta t_2, \dots, \Delta t_N] \quad (3)$$

Note that the possible focussing range is limited. It involves the range from the near field length of a single element to the near field length of the whole array.

#### B. Determination of average sound velocity

The determination of the average sound velocity works by the following steps:

- choosing a time frame at an arbitrary position of the signal with a width of about  $1 \mu s$
- determination of the time of flight  $t_{max}$  where the signal, emitted and received with the central element, has its maximal amplitude
- assumption of a (reasonable) testing sound velocity  $c_{Test}$  and of the corresponding position of the scatterer  $z_{Test} = c_{Test} t_{max}/2$
- focussing all signals using (1) with the parameters  $z_{Test}$  and  $c_{Test}$  and determination of resulting signal energy as well as the resulting signal amplitude

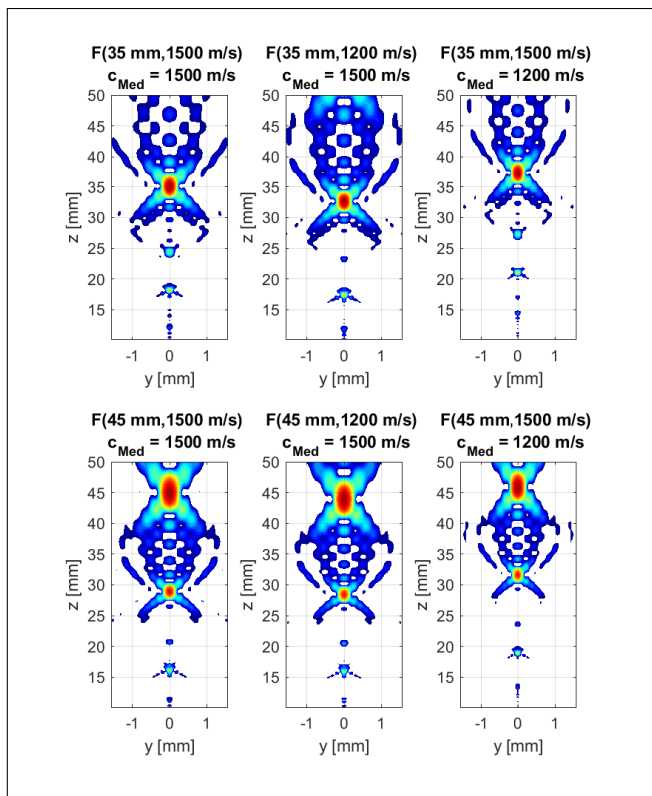


Figure 7. Calculated sound fields for focussing in to different depth; top: 35 mm, bottom: 45 mm, for different media und different focussing regimes

- variation of  $c_{Test}$  and taking up signal energy  $E(c_{Test})$  and Amplitude  $A(c_{Test})$  as a function of the testing sound velocity
- determination of the correct average sound velocity by determining the maximum of both of the curves  $c_{med,A} = \text{argmax}(A(c_{test}))$ ,  $c_{med,E} = \text{argmax}(E(c_{test}))$
- plausibility check via comparing the maximal amplitude  $A_{max}$  with the averaged amplitude  $\bar{A}$  and the requirement  $A_{max} > 2\bar{A}$  (if only noise is evaluated they will be nearly similar)
- stepwise shifting of the time frame through the recorded signal and determination of the average sound velocity  $c_{av,i}$  locally resolved.

The width of the time frame is determined by the demand that the frame should be much longer than the signal length of about  $0.4 \mu s$  but not that large, that several echoes are in one window. Also the testing sound velocities should be in a reasonable range. As the sound velocity of tissue is in a range of  $1500 m/s$  to  $1700 m/s$  values below  $1000 m/s$  or above  $2500 m/s$  are not useful.

Figure 8 shows an example of a resulting curve of determined signal energy versus testing sound velocity. If there are not sufficient scatterers in the frame, the resulting energy is nearly constant and there is no significant maximum. In this case, the determined sound velocity is neglected.

After determining the correct average sound velocities  $c_{av,i}$  for each frame position, the position  $z_i$  of the scattering algae

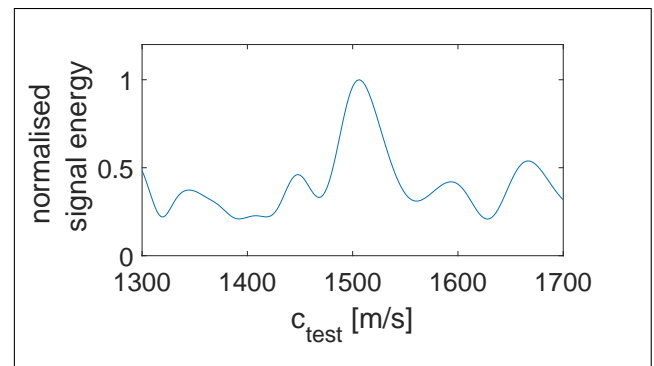


Figure 8. Evaluation of the resulting signal energy as a function of the used testing sound velocity.

can be determined. The value of  $c_{av,i}$  is the average sound velocity from the transducer to the corresponding focus depth. To determine the local sound velocity, which is only averaged from one position to the next, (4) can be used:

$$c_{loc,i} = \frac{c_{av,i}z_i - c_{av,i-1}z_{i-1}}{z_i - z_{i-1}} \quad (4)$$

To determine the temperature distribution additionally, only the dependence of sound velocity from temperature is needed.

#### IV. RESULTS

Figure 9 shows a determined sound velocity profile with sound velocity versus time of flight (top) and sound velocity versus reflector position (bottom). As this is a measurement for constant temperature (and so for constant sound velocity), the observable deviations can be interpreted as the uncertainty of the technique. The measurement uncertainty is about  $\pm 15 m/s$  or 2%, independent if signal energy or signal amplitude are evaluated.

After validating the measurement technique for constant sound velocities, it shall be used to monitor a heating process. The experimental set-up shown in Figure 4 was used to generate a temperature gradient. Measurements were starting with switching on the heat source. One measure was started each 20 s and the introduced algorithm was applied on the measured data. The results are shown in Figure 10. Each column of the picture represents one reconstructed sound velocity profile as it is shown in Figure 9, whereby the sound velocity is colour-coded. So, the  $y$ -axis represents the measuring depth and it is directed in a way that the heat source and the transducer would be above and the cooling would be below the picture. The  $x$ -axis represents the progressing duration of the measurements. It is easily notable that a sound velocity gradient appears with increasing measurement duration. Note that there is already a small gradient when the measurement starts. The reason is that the bottom is kept to  $4^\circ C$  whereas the top of the gel-phantom has room temperature of about  $20^\circ C$ .

#### V. CONCLUSION

This contribution introduced and qualified a new measurement technique to measure temperatures respectively sound velocity locally and temporarily resolved in tissue phantoms. As an absolute value for the sound velocity is measured, it is not only possible to determine a relative change of temperature,

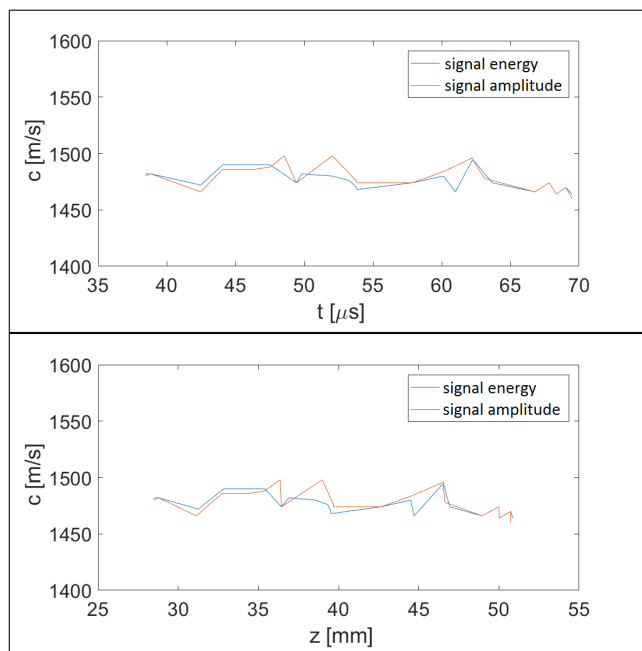


Figure 9. Reconstructed sound velocity profiles, evaluating signal energy (blue) and signal amplitude (red); top: sound velocity versus time of flight, bottom: sound velocity versus measurement depth

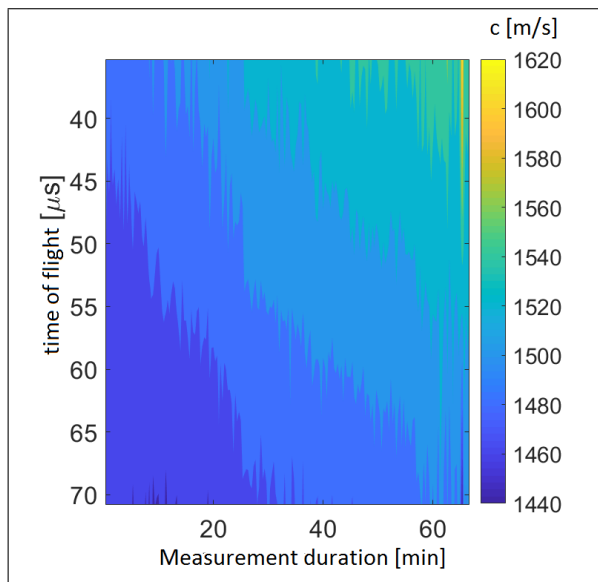


Figure 10. Resulting monitored temperature profile; colour-coded: determined sound velocity, *y*-axis: time of flight respectively measurement depth, *x*-axis: duration of the measurements.

like in the classic approach, but it is possible to relate the temperature to fixed measurement positions. The technique works independently of the thermal expansion of the tissue.

Currently, the measurement uncertainty of the technique is about 2% the reachable local resolution is about 1 mm at 10 MHz. The temporal resolution depends on the total duration of the experiment. For durations of a few minutes it is possible to measure each second. For longer experiments a measure can be performed each 20 s. It is mainly limited by memory capacity and by the available data transfer rates of the measurement hardware.

To improve the reachable accuracy, examination of the used focussing regimes are necessary. Improved regimes result in a smaller focus area, so that the evaluation algorithm is more sensitiv to the sound velocity.

Enhancing the signal to noise ratio of the used electronics, especially of the amplifiers in the receive channels, allows to reduce the necessary number of averaged signals and so to enhance the possible temporal resolution. Examinations with transducers with another frequency range are planned to examine the relation between frequency and local resolution.

ACKNOWLEDGMENT

The authors would like to thank the Deutsche Forschungsgemeinschaft (DFG) for the financial support in the ongoing project: 260366138, and SONAXIS for developing and manufacturing the array transducer for high temperatures.

REFERENCES

- [1] G. Shen, Y. Chen, and G. Ren, "An improved tumour temperature measurement and control method for superficial tumour ultrasound hyperthermia therapeutic system," in Journal of Physics: Conference Series, vol. 48, no. 1. IOP Publishing, 2006, p. 653.
- [2] H.-Y. Tseng, G.-B. Lee, C.-Y. Lee, Y.-H. Shih, and X.-Z. Lin, "Localised heating of tumours utilising injectable magnetic nanoparticles for hyperthermia cancer therapy," IET nanobiotechnology, vol. 3, no. 2, 2009, pp. 46–54.
- [3] D. A. Iero, L. Crocco, and T. Isernia, "Thermal and microwave constrained focusing for patient-specific breast cancer hyperthermia: A robustness assessment," IEEE Transactions on Antennas and Propagation, vol. 62, no. 2, 2014, pp. 814–821.
- [4] A. Anand, D. Savary, and C. Hall, "Three-dimensional spatial and temporal temperature imaging in gel phantoms using backscattered ultrasound," IEEE transactions on ultrasonics, ferroelectrics, and frequency control, vol. 54, no. 1, 2007, pp. 23–31.